01 Oct 1976

Excitation of the n=2 State of Atomic Hydrogen by Electron Impact in the Distorted-Wave Approximation

Ralph V. Calhoun

Don H. Madison
Missouri University of Science and Technology, madison@mst.edu

W. Neil Shelton

Recommended Citation

R. V. Calhoun et al., "Excitation of the n=2 State of Atomic Hydrogen by Electron Impact in the Distorted-Wave Approximation," *Physical Review A - Atomic, Molecular, and Optical Physics*, vol. 14, no. 4, pp. 1380-1387, American Physical Society (APS), Oct 1976.
The definitive version is available at https://doi.org/10.1103/PhysRevA.14.1380

PHYSICAL REVIEW A VOLUME 14, NUMBER 4 OCTOBER 1976

Excitation of the $n = 2$ state of atomic hydrogen by electron impact in the distorted-wave approximation

Ralph V. Calhoun and D. H. Madison
Department of Physics, Drake University, Des Moines, Iowa 50311

W. N. Shelton
Department of Physics, The Florida State University, Tallahassee, Florida 32306

(Received 19 April 1976)

The differential cross sections for excitation of the $n = 2$ state of atomic hydrogen by the impact of electrons with energies of 54, 100, 136, and 200 eV are calculated in the distorted-wave approximation with exchange included. Cross sections for excitation of the $2s_{1/2}$, $2p_{1/2}$, and $2p_{3/2}$ states are calculated and summed to give the $n = 2$ differential cross sections. The results of this calculation are compared with previous theoretical calculations and with recent absolute experimental data.

I. INTRODUCTION

The calculation of differential cross sections for low-energy electron-impact excitation of atoms has been the subject of much theoretical work. The results, however, are still not in satisfactory agreement with the experimental data. Since electron-impact excitation of atomic hydrogen is one of the simplest inelastic scattering processes, it provides a basis for accurate comparison of available theories. Due to the fact that exact wave functions and potentials are known for atomic hydrogen, fundamental differences in the various scattering approximations may be directly studied. Comparisons of various theories for other scattering problems are often complicated by the use of different bound-state wave functions and potentials. There have been many papers written on the electron-hydrogen problem.[1,2] No attempt is made to include comparisons to all the available calculations. We have attempted to select a representative sampling of these works for comparison with the present calculation.

The cross sections studied in this work are for the energy range 54–200 eV. In this energy range, coupling due to participation of intermediate states may be reasonably neglected, although this coupling becomes increasingly important as one approaches threshold energies. Consequently, approximations which consider only coupling of the initial and final states need to be considered. The usefulness of more elementary approximations, such as the Born approximation, are severely limited for these energies. Since the Born approximation is valid only for small-momentum transfer, it gives reasonable differential cross sections only for a small angular range in the forward direction. If one is not interested in the detailed nature of the angular distributions but rather in the total cross sections integrated over all angles, then the Born approximation is sufficient for intermediate and high energies. This is readily evident since the major contribution to the total cross section comes from the small-angle region. The ease of calculation using the Born approximation is a most favorable characteristic, and is responsible for the approximation's popularity.

The electron-atom scattering problem is complicated by two factors: the possibility of interchange of continuum and atomic electrons, and the polarization of the atomic charge distribution due to the presence of the continuum electron. The distorted-wave approximation (DWA) takes into account the distortion of the scattered wave by the atomic potential. This distortion becomes increasingly important as the energy of the incident electron is decreased. Provision is also made for the possibility of interchange of atomic and continuum electrons in the DWA. It would be reasonable to conclude, *a priori*, that an approximation, such as the DWA, would yield superior cross sections to those obtained with plane-wave theories. While the DWA calculation lacks the compactness of an analytical expression, it does present a numerical problem which is easily solved with the aid of high-speed computers.

In this work differential cross sections are calculated for excitation of both the $2s$ and $2p$ shells and these cross sections are summed to give the total $n = 2$ differential cross sections. In an earlier work, the $2s$ cross sections were calculated by Shelton *et al.*[3] and Shelton and Mix[4] using the DWA. At that time, experimental absolute differential cross sections for the $2s$ excitation were not available. The summed $2s$ and $2p$ differential cross sections of the present work are compared to the recently available $n = 2$ absolute experimental cross sections of Williams and Willis.[2] These experi-

mental cross sections were obtained by measuring in coincidence the angular distributions of the 10.2-eV photons and the electrons with a 10.2-eV energy loss. Comparisons between the DWA and this experimental data are made at 54, 100, 136, and 200 eV.

The results of the present work are also compared to the theoretical calculations of Gau and Macek,[5] who used an extended Glauber approximation, the distorted-wave polarized-orbital calculation of McDowell *et al.*,[6] and the Glauber approximation of Thomas and Gerjuoy.[7]

A distorted-wave calculation similar to the one discussed here has been reported by Thomas *et al.*[8] for excitation of helium using the random-phase Approximation. No calculations of this type have been reported for excitation of hydrogen. However, based upon the helium results, one would expect such a calculation to give results very similar to those reported here except at low energies where the angular distributions are more sensitive to the atomic potential. The Coulomb-projected Born calculation of Geltman and Hildalgo[9] does not reproduce the data as well as the present calculation.

After submission of this manuscript, the close-coupling results of Kingston, Fon, and Burke[10] became available. A comparison is also made to their work as it represents a major improvement in the agreement between experimental results and the calculations of Ref. 5–7. In this calculation, the well known close-coupling approximation as described by Burke and Schey[11] is used to calculate the T matrix for the lower partial waves and the Born approximation is used to calculate the higher partial waves needed for convergence. A similar calculation was performed by Brandt and Truhlar[12] to calculate the $1s$-$2p$ cross sections for energies up to 54 eV.

II. DISTORTED-WAVE THEORY

The formal theory of the DWA is developed in standard texts on scattering theory.[13,14] The DWA as it is applied to the electron-hydrogen problem is given as follows. The interaction of the continuum electron with the atom is expressed as the sum of the two potentials,

$$V_I = V_0 + V_1. \tag{1}$$

In the DWA, the T matrix for the transition from the initial to final state may be approximated as

$$T_{ba} = \langle \chi_b^{(-)}(1)\psi_B(2) \,|\, V_0(1-P_{12}) \,|\, \chi_a^{(+)}(1)\psi_A(2)\rangle + \langle \chi_b^{(-)}(1)\psi_B(2) \,|\, V_1(1-P_{12}) \,|\, \chi_a^{(+)}(1)\psi_A(2)\rangle, \tag{2}$$

where (1) and (2) refer to the coordinates of the continuum and atomic electron, respectively. The wave function $\psi_{A(B)}(2)$ represents the initial (final) state of the atomic electron, and $\chi_{a(b)}(1)$ represents the continuum electron in the incident (exit) channel. The operator P_{12} interchanges electrons 1 and 2. For the present case, V_0 is taken as the interaction with the static atomic potential of the hydrogen atom in the $1s$ state,

$$V_0 = -2[(1+r_1)/r_1]e^{-2r_1} \tag{3}$$

expressed in rydbergs. The interaction potential V_I, which is the interaction of the continuum electron with the atom is given by

$$V_I = 2/r_{12} - 2/r_1. \tag{4}$$

The second term in Eq. (4) represents the interaction of the continuum electron with the atomic nucleus and is known as the core term. Since V_I is given by Eq. (1), V_1 must be

$$V_1 = V_I - V_0 = 2/r_{12} - 2/r_1 + 2[(1+r_1)/r_1]e^{-2r_1}. \tag{5}$$

The terms involving the single coordinate r_1 do not contribute to the integral in Eq. (2) due to the orthogonality of the initial and final states.[15]

The distorted waves, or continuum wave functions, represent elastic scattering states, and are solutions to the equation

$$(\nabla^2 + k^2 + V_0)\chi^{(+)}(r_1) = 0, \tag{6}$$

where k^2 is the projectile energy in rydbergs and k is the wave number. The solution of Eq. (6) is obtained by numerical integration and then matched to the proper combination of phase-shifted spherical Bessel functions at large r_1 to assure the proper asymptotic behavior.

After applying orthogonality conditions, the T matrix reduces to

$$T_{ba} = \langle \chi_b^{(-)}(1)\psi_B(2) \,|\, (2/r_{12})(1-P_{12}) \,|\, \chi_a^{(+)}(1)\psi_A(2)\rangle. \tag{7}$$

The T matrix may be evaluated by making a partial wave expansion of the distorted waves, and a multipole expansion of $2/r_{12}$. The plane-wave-normalized expansion of the distorted wave is

$$\chi_a^{(+)}(1) = \frac{4\pi}{k_a r_1} \sum_{l_a j_a m_1} i^{l_a} \chi_{l_a j_a}(k_a r_1) \times C(l_a s_a j_a; m_1, m_a, m_1 + m_a) \times Y_{l_a}^{m_1 *}(\Omega_{k_a}) Y_{l_a}^{m_1}(\Omega_1) \,|\, s_a m_a\rangle, \tag{8}$$

where $|s_a m_a\rangle$ is a spinor. The radial part of the distorted wave has the asymptotic form

$$\chi_{lj}(kr) \to e^{i\delta_{lj}} \sin(kr - \tfrac{1}{2}l\pi + \delta_{lj}). \tag{9}$$

And the bound-state wave function is expressed as

$$\psi_A(2) = \sum_{M_L M_S} C(LSJ_A; M_L M_S M_A) i^{L_A} \frac{U_{nL_A}(r_2)}{r_2} Y_{L_A}^{M_L}(\Omega_2). \tag{10}$$

The T matrix may thus be reduced to a radial part which is integrated numerically and to an angular part which is handled by standard angular momentum techniques. The transferred angular momentum consists of spin and orbital momentum. Since the assumed interaction is spin independent, spin may be transferred to the atom only in the exchange scattering process. The total angular momentum transferred to the atom is the difference of the initial and final total atomic angular momentum,

$$\vec{j} = \vec{J}_B - \vec{J}_A. \tag{11}$$

It can be shown that an expansion of the T matrix in terms of the angular momentum transferred can be written as[15]

$$T_{ba} = \sum_{lsj} C(J_A j J_B; M_A, M_B - M_A, M_B)\beta_{sj}^{lmm_b m_a}(\vec{k}_b, \vec{k}_a), \tag{12}$$

where β is given by

$$\beta_{sj}^{lmm_b m_a} = \sum_{\substack{l_a j_a m_1 \\ l_b j_b}} 4\pi I_{l_b j_b l_a j_a}^{lsj} i^{l-l_a-l_b}\hat{\hat{l}}\hat{\hat{s}}\hat{\hat{j}}_b C(l_b s_b j_b; m_1 - m, m_b, m_b + m_1 - m) C(l_a s_a j_a; m_1, m_a, m_1 + m_a)$$

$$\times C(j_b j j_a; m_1 + m_b - m, m - m_b + m_a, m_1 + m_a) X(l_a s_a j_a; l_b s_b j_b; lsj) Y_{l_a}^{m_1}(\Omega_{k_a}) Y_{l_b}^{m_1 - m}(\Omega_{k_b}). \tag{13}$$

The quantity $\hat{f} \equiv (2f+1)^{1/2}$, while X is a Fano coefficient.[16] The radial integral in Eq. (13) is

$$I_{l_b j_b l_a j_a}^{lsj} = \frac{4\pi}{k_a k_b} \int_0^\infty dr_1 \int_0^\infty dr_2 \chi_{l_b j_b}(k_b r_1) \chi_{l_a j_a}(k_a r_\alpha) G_{l l_b l_a}^{sj}(r_1, r_2). \tag{14}$$

The radial part of the atomic wave function is contained in the function G. Using L, S, and J to represent the orbital, spin, and total angular momentum of the atomic electron, G for hydrogen becomes

$$G_{l l_b l_a}^{sj}(r_1, r_2) = \sum \hat{L}_A \hat{L}_B \hat{J}_A \hat{s}_b \hat{l}_a \hat{j}_b \hat{l}^{-1} i^{l-L_A-L_B} \Bigg(W(L_B l S_A J_A; L J_B) C(l_a l_b l; 000) C(L_A L_B l; 000) U_{nL_A}(r_2) U_{n'L_B}(r_2)$$

$$\times \frac{2}{2l+1} \frac{r_<^l}{r_>^{l+1}} \delta_{\alpha 1} - \frac{\hat{S}\hat{S}_A}{2} \hat{S}_B \hat{l} \hat{j} X(L_A l L_B; S_A S S_B; J_A j J_B)$$

$$\times \sum_K (-)^K \hat{K}^2 W(L_A l_b L_B l_a; K l) C(L_B K l_a; 000)$$

$$\times C(L_A K l_b; 000) U_{n'L_B}(r_2) U_{nL_A}(r_1) \frac{2}{2K+1} \frac{r_<^K}{r_>^{K+1}} \delta_{\alpha 2} \Bigg). \tag{15}$$

The first term in Eq. (15) is the direct part of T matrix and the second term is the exchange term. In the exchange term, the coordinates of the radial wave functions for the free and atomic electrons are interchanged. The symbol W is a Racah coefficient,[17] and U_{nL} represents the radial part of the bound-state hydrogen wave function.

The differential cross section for unpolarized beams incident upon unpolarized targets with initial (final) angular momentum $J_A(J_B)$ is expressed in terms of the T matrix as

$$\frac{d\sigma}{d\Omega}(J_A \to J_B) = \frac{1}{16\pi^2} \frac{k_b}{k_a} \hat{J}_A^{-2} \hat{S}_A^{-2} \sum_{\substack{M_A M_B \\ m_a m_b}} |T_{ba}|^2. \tag{16}$$

Using Eq. (12) in the above equation, the differential cross section becomes

$$\frac{d\sigma}{d\Omega}(J_A \to J_B) = \frac{1}{16\pi^2} \frac{k_b}{k_a} \frac{\hat{J}_B^2}{\hat{J}_A^2 \hat{S}_A^2} \sum_{j m m_b m_a} \Big| \sum_{ls} \beta_{sj}^{lmm_b m_a} \Big|^2. \tag{17}$$

It is important to note that the differential cross section consists of a coherent sum of the multipoles of various l and s transfer, but an incoherent sum of multipoles of different j transfer. The possible triads of l, s, j available for the $2s_{1/2}$, $2p_{1/2}$, and $2p_{3/2}$ transitions are given in Table I. Transitions with $s = 1$ can occur only by means of the exchange process. Since spin-orbit coupling is weak for atomic hydrogen, the $2p_{1/2}$ and $2p_{3/2}$ cross sec-

TABLE I. Allowed values of angular momentum transfer (l, s, j) for the $s_{1/2}$, $p_{1/2}$, and $p_{3/2}$ transitions.

Transition	l	s	j	Process
$1s_{1/2} \to 2s_{1/2}$	0	0	0	Direct and exchange
	0	1	1	Exchange
$1s_{1/2} \to 2p_{1/2}$ or $2p_{3/2}$	1	0	1	Direct and exchange
	1	1	1	Exchange
	1	1	0	Exchange ($2p_{1/2}$ only)
	1	1	2	Exchange ($2p_{3/2}$ only)

tions are related in the following way:

$$\frac{d\sigma}{d\Omega}(1s_{1/2} \rightarrow 2p_j) \cong \frac{2j+1}{2j'+1} \frac{d\sigma}{d\Omega}(1s_{1/2} \rightarrow 2p_{j'}). \quad (18)$$

Therefore, the $1s \rightarrow 2p_{3/2}$ cross section is twice the $1s \rightarrow 2p_{1/2}$ cross section. The cross sections for the $1s \rightarrow 2p_{1/2}$ and $1s \rightarrow 2p_{3/2}$ were then summed to give the $1s \rightarrow 2p$ cross sections. The total $n = 2$ differential cross section is the incoherent sum of the $1s \rightarrow 2s$ and $1s \rightarrow 2p$ cross sections.

III. NUMERICAL METHODS

Differential cross sections for hydrogen were calculated using a CDC 6400. The radial parts of the distorted waves were obtained by numerical integration of the Schrödinger equation using Noumerov's method.[18] The integration was performed on a step size of initially $0.0022a_0$ which was doubled after every 40 mesh points until the k^2 term in Eq. (6) began to dominate the V_0 term, after which the step size was maintained constant.

The double integrations in Eq. (14) were performed using Simpson's method. The integrations were carried out over the interval from the origin out to $181a_0$ for the $2p$ excitation and out to $22a_0$ for the $2s$ excitation. The number of partial waves calculated numerically varied with energy according to $l \approx 10$ k. However, more partial waves were needed to obtain suitable convergence for the $2p$ transition, and additional partial waves up to $l = 350$ were calculated analytically.[15]

IV. RESULTS

The DWA differential cross sections for the $2s$, $2p$, and $2s + 2p$ excitation are displayed graphically in Figs. 1–4, and tabulated in Tables II–V. The experimental data are those of Ref. 2. At small angles, the $2p$ cross sections provide the major contribution to the total differential cross sections. The $2s$ and $2p$ cross sections approach the same order of magnitude only for angles greater than 30°. Therefore, the total $n = 2$ cross sections, integrated over all angles, is determined by the $2p$ contribution. Overall, the agreement between the DWA cross sections and the experimental data is qualitatively good.

DWA $1s$-$2s$ cross sections were obtained in the earlier work of Shelton *et al.*[3] In that work the distorted waves for the incident and exit channels were calculated as eigenfunctions of the ground-state and excited-state potentials, respectively. In this work, all continuum wave functions were calculated as eigenstates of the ground-state potential. These two approaches give $2s$ cross sections that differ slightly at large angles. The present

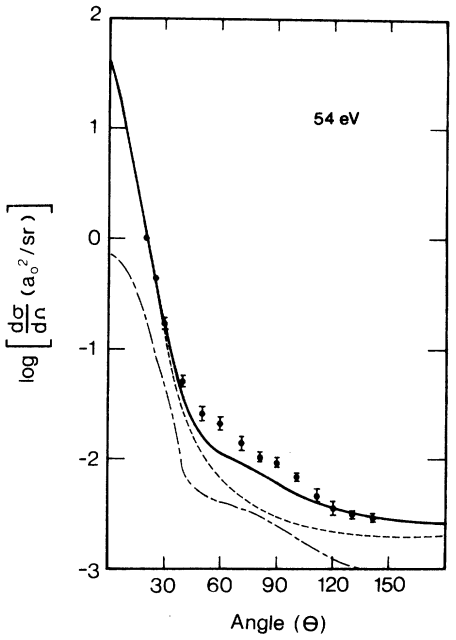

FIG. 1. Differential cross section for (a) – – – –, $1s - 2p$; (b) — — —, $1s - 2s$; and (c) ——, $1s - 2s + 2p$ excitation of hydrogen in units of a_0^2 at 54 eV. The experimental data ♦ are those of Ref. 2.

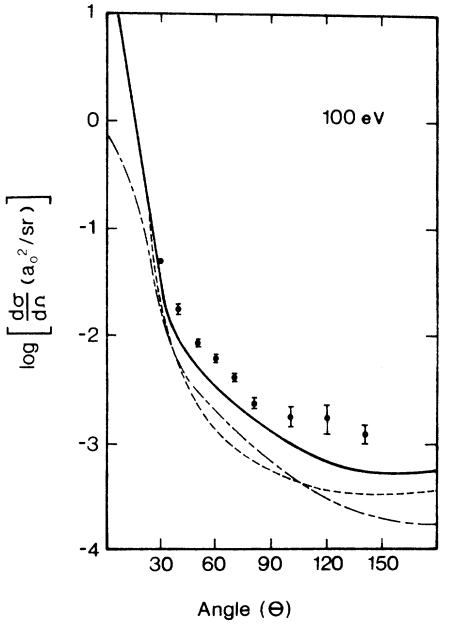

FIG. 2. Differential cross section for (a) – – – –, $1s - 2p$; (b) — — —, $1s - 2s$; and (c) ——, $1s - 2s + 2p$ excitation of hydrogen in units of a_0^2 at 100 eV. The experimental data ♦ are those of Ref. 2.

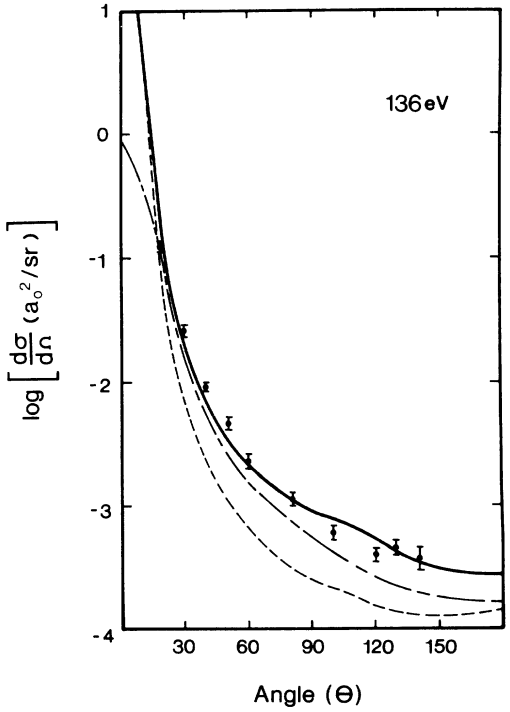

FIG. 3. Differential cross section for (a) – – – –, $1s-2p$; (b) — — —, $1s-2s$; and (c) ——, $1s-2s+2p$ excitation of hydrogen in units of a_0^2 at 136 eV. The experimental data ✦ are those of Ref. 2.

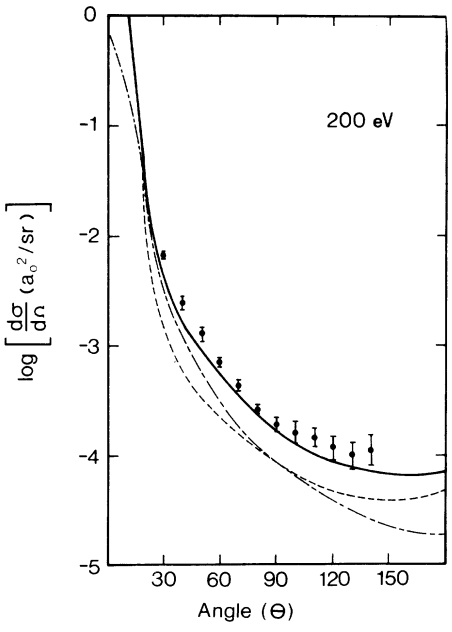

FIG. 4. Differential cross section for (a) – – – –, $1s-2p$; (b) — — —, $1s-2s$; and (c) ——, $1s-2s+2p$ excitation of hydrogen in units of a_0^2 at 200 eV. The experimental data ✦ are those of Ref. 2.

TABLE II. Differential cross sections (a_0^2 sr^{-1}) for electron impact excitation of the $n=2$ state of hydrogen at 54 eV.[a]

Angle (deg)	2s	2p	2s+2p
0	7.30 (–1)	4.44 (1)	4.51 (1)
15	3.40 (–1)	3.08 (0)	3.42 (0)
30	4.49 (–2)	1.58 (–1)	2.03 (–1)
45	5.65 (–3)	1.48 (–2)	2.05 (–2)
60	4.30 (–3)	6.43 (–3)	1.07 (–2)
75	3.51 (–3)	4.38 (–3)	7.89 (–3)
90	2.48 (–3)	3.21 (–3)	5.69 (–3)
105	1.70 (–3)	2.55 (–3)	4.25 (–3)
120	1.20 (–3)	2.21 (–3)	3.41 (–3)
135	8.96 (–4)	2.09 (–3)	2.99 (–3)
150	7.20 (–4)	2.20 (–3)	2.91 (–3)
165	6.31 (–4)	2.43 (–3)	3.06 (–3)
180	5.96 (–4)	2.52 (–3)	3.11 (–3)

[a] Numbers in parentheses refer to powers of ten.

computer code was checked by reproducing the results of the earlier calculation.

In Figs. 5–7, the total $n=2$ DWA differential cross sections are compared to the theoretical calculations of Refs. 5–7, and also to a plane-wave calculation performed by the present authors. As discussed previously, a plane-wave theory such as the Born approximation should not give proper cross sections for the entire angular range. A comparison is made nevertheless, since the Born approximation is a popular standard. To account for the possibility of interchange of atomic and continuum electrons the Born-Oppenheimer[19] approximation is used to calculate the exchange am-

TABLE III. Differential cross sections (a_0^2 sr^{-1}) for electron impact excitation of the $n=2$ state of hydrogen at 100 eV.[a]

Angle (deg)	2s	2p	2s+2p
0	8.49 (–1)	9.76 (1)	9.84 (1)
15	2.34 (–1)	1.16 (0)	1.39 (0)
30	1.51 (–2)	1.95 (–2)	3.46 (–2)
45	3.32 (–3)	2.25 (–3)	5.57 (–3)
60	1.87 (–3)	1.37 (–3)	3.24 (–3)
75	1.08 (–3)	8.84 (–4)	1.96 (–3)
90	6.54 (–4)	6.02 (–4)	1.25 (–3)
105	4.27 (–4)	4.61 (–4)	8.88 (–4)
120	3.04 (–4)	3.67 (–4)	6.71 (–4)
135	2.34 (–4)	3.22 (–4)	5.56 (–4)
150	1.96 (–4)	3.26 (–4)	5.22 (–4)
165	1.77 (–4)	3.63 (–4)	5.40 (–4)
180	1.70 (–4)	3.12 (–4)	4.82 (–4)

[a] Numbers in parentheses refer to powers of ten.

TABLE IV. Differential cross sections (a_0^2 sr^{-1}) for electron impact excitation of the $n = 2$ state of hydrogen at 136 eV.[a]

Angle (deg)	2s	2p	2s +2p
0	9.03 (−1)	9.41 (2)	9.42 (2)
15	2.13 (−1)	6.07 (−1)	8.20 (−1)
30	1.72 (−2)	6.15 (−3)	2.34 (−2)
45	3.39 (−3)	1.06 (−3)	4.45 (−3)
60	1.55 (−3)	6.63 (−4)	2.21 (−3)
75	8.70 (−4)	3.59 (−4)	1.12 (−3)
90	5.74 (−4)	2.54 (−4)	8.28 (−4)
105	3.61 (−4)	1.99 (−4)	5.65 (−4)
135	2.04 (−4)	1.43 (−4)	3.47 (−4)
150	1.85 (−4)	1.16 (−4)	3.01 (−4)
165	1.72 (−4)	1.13 (−4)	2.85 (−4)
180	1.36 (−4)	1.47 (−4)	2.83 (−4)

[a] Numbers in parentheses refer to powers of ten.

plitude. The interaction potential used in this calculation represents the interaction of the continuum electron with the atomic electron excluding the core term. The resultant Born-Oppenheimer–minus-core (BOMC) approximation provides a variation of the ordinary Born approximation which is consistent with the assumptions made for the DWA calculation. Distortion of the continuum wave function, however, is not included in the BOMC. As can be seen in Figs. 5–7, the BOMC curve matches the shape of the experimental data only for relatively small angles and fails by several orders of magnitude for the larger angles. The Glauber approximation of Ref. 7 and the extended Glauber approximation of Ref. 5 give cross sections which are substantially in better agreement with the experimental data than the BOMC curves, but still do not give proper cross sections at the larger angles. The extended Glauber approximation of Gau and Macek[5] differs from the conventional Glauber approximation by not restricting the momentum transfer to the transverse direction. Their differential cross sections, however, are somewhat less satisfactory than are the cross sections obtained with the conventional Glauber approximation. In the distorted-wave polarized-orbital-II (DWPOII) calculation of McDowell *et al.*[6] polarization of the atomic target is included in the incident channel and the incident channel continuum wave corresponds to an adiabatic-exchange function.

TABLE V. Differential cross sections (a_0^2 sr^{-1}) for electron impact excitation of the $n = 2$ state of hydrogen at 200 eV.[a]

Angle (deg)	2s	2p	2s +2p
0	9.16 (−1)	2.13 (2)	2.14 (2)
15	9.21 (−2)	2.24 (−1)	3.16 (−1)
30	2.78 (−3)	1.40 (−3)	4.18 (−3)
45	8.00 (−4)	3.86 (−4)	1.19 (−3)
60	3.46 (−4)	2.37 (−4)	5.83 (−4)
75	1.68 (−4)	1.19 (−4)	2.87 (−4)
90	9.27 (−5)	8.54 (−5)	1.78 (−4)
105	5.78 (−5)	6.81 (−5)	1.26 (−4)
135	3.04 (−5)	4.82 (−5)	7.86 (−5)
150	2.53 (−5)	3.55 (−5)	6.08 (−5)
165	2.30 (−5)	3.49 (−5)	5.79 (−5)
180	2.14 (−5)	5.68 (−5)	7.82 (−5)

[a] Numbers in parentheses refer to powers of ten.

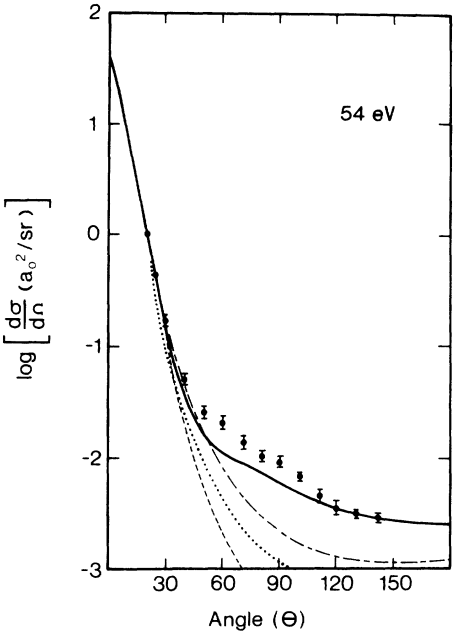

FIG. 5. Differential cross section calculated with (a) ——, DWA; (b) – – – –, BOMC; (c) —+—, Glauber; (d) ·····, extended Glauber (Gau and Macek); and (e) — – —, DWPOII for $1s - 2s + 2p$ excitation of hydrogen in units of a_0^2 at 54 eV. The experimental data ♣ are those of Ref. 2.

For the angular range of 0°–30°, all of the approximations discussed above produce cross sections of approximately the same shape and magnitude. This can be attributed to the dominance of the $2p$ contribution to the total differential cross section, and the validity of the Born approximation for s-to-p transitions in the region of small-momentum transfer. All should give total integrated cross sections of the same approximate value for this reason.

For angles greater than 30°, the DWA cross sec-

tions are in better agreement with the experimental data than the Glauber and DWPOII theories. At 200 eV, the DWA cross sections are in almost complete agreement with the experimental data for the entire angular range. None of the approximations discussed produce angular distributions which have the proper behavior at intermediate to large angles. The Glauber approximation of Thomas and Gerjuoy gives cross sections which are consistently better than those obtained using either the extended Glauber approximation or the DWPOII approximation. Their prediction for 200 eV is, nonetheless, approximately three times too small at 120°.

In Fig. 8, the $1s$-$2s$ and $1s$-$2p$ differential cross sections calculated with the DWA and the close-coupling method of Ref. 10 are compared. It is interesting to note that their $1s$-$2s$ cross section is larger than the DWA $1s$-$2s$ cross section at forward and back angles. However, their $1s$-$2p$ cross sections are smaller than the DWA $1s$-$2p$ cross sections in these regions. The differences between these two calculations are effectively canceled

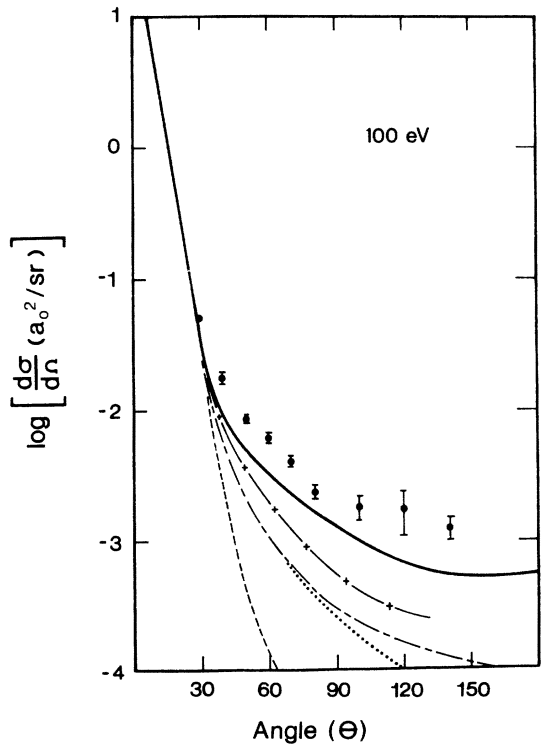

FIG. 6. Differential cross section calculated with (a) ——, DWA; (b) – – – –, BOMC; (c) —+—, Glauber; (d) ·····, extended Glauber (Gau and Macek); and (e) — – —, DWPOII for $1s-2s+2p$ excitation of hydrogen in units of a_0^2 at 100 eV. The experimental data ♦ are those of Ref. 2.

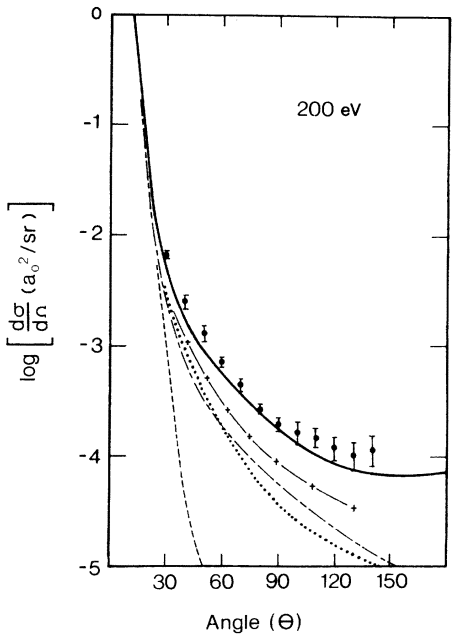

FIG. 7. Differential cross section calculated with (a) ——, DWA; (b) – – – –, BOMC; (c) —+—, Glauber; (d) ·····, extended Glauber (Gau and Macek); and (e) — – —, DWPOII for $1s-2s+2p$ excitation of hydrogen in units of a_0^2 at 200 eV. The experimental data ♦ are those of Ref. 2.

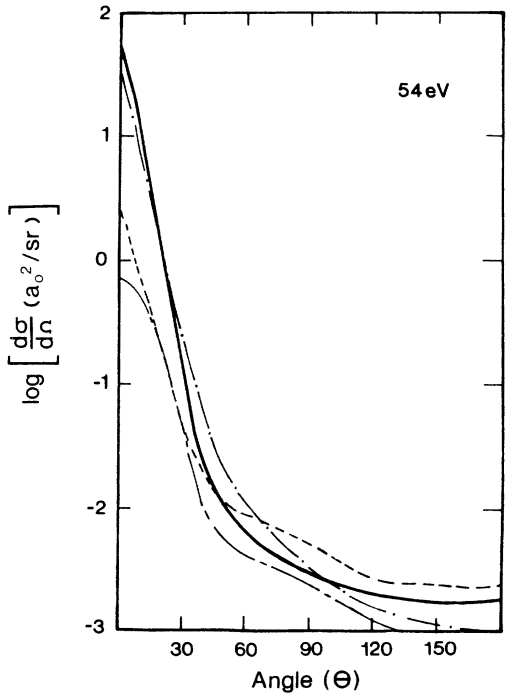

FIG. 8. Differential cross sections for (a) ——, $1s-2p$; (b) – – –, $1s-2s$ excitation calculated with the DWA; and (c) —·—, $1s-2p$; (d) – – – – –, $1s-2s$ excitation calculated with the close-coupling method of Ref. 7 for 54 eV in units of a_0^2.

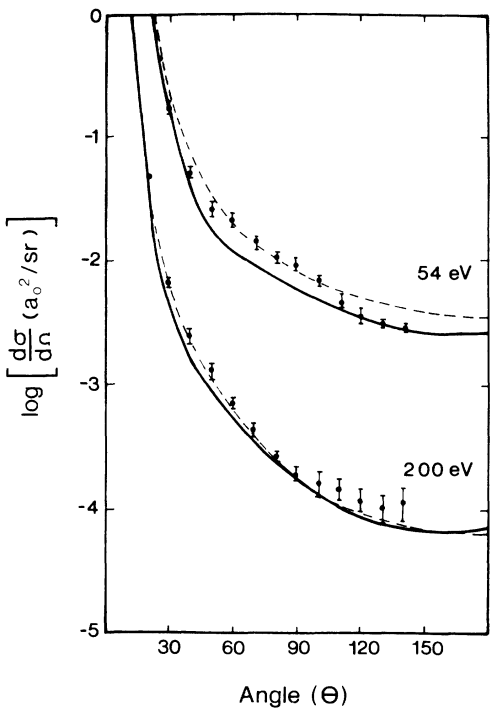

FIG. 9. Differential cross sections calculated with (a) ——, the DWA and (b) - - - - - -, the close-coupling method of Ref. 7 for $1s - 2s + 2p$ at 54 and 200 eV in units of a_0^2. The experimental data ♦ are those of Ref. 2.

when a sum is taken. The $1s - 2s + 2p$ cross sections calculated with the close-coupling method are compared with the DWA cross sections at 54 and 200 eV in Fig. 9. Both agree reasonably well with the experimental data of Ref. 2. The close-coupling calculation is in slightly better agreement with this data in the 30°–90° angular range than is the DWA calculation.

TABLE VI. Total integrated cross sections (a_0^2) for electron impact excitation of the $n = 2$ state of hydrogen.

Energy (eV)	$1s \rightarrow 2s$	$1s \rightarrow 2p$	$1s \rightarrow 2s + 2p$
54	0.239	3.039	3.278
100	0.161	2.271	2.432
136	0.088	1.845	1.933
200	0.087	1.308	1.395

The integrated cross sections, calculated in the DWA, are shown in Table VI. Approximately 93% of the $n = 2$ integrated cross section comes from the $1s \rightarrow 2p$ cross section. The $1s \rightarrow 2s$ process is responsible for only (6–7)% of the total cross section at these energies, due to its relatively small value at forward angles.

Work is presently underway to calculate amplitudes for the excitation of the magnetic sublevels of the $n = 2$ states of atomic hydrogen. These amplitudes cannot be extracted directly from the present calculation since the T matrix is expanded in multipoles of the total angular momentum transfer. However, since the spin-orbit coupling is very weak, the various multipoles given in Eq. (13) may be recoupled to give the appropriate amplitudes. Comparison of the magnetic sublevels obtained in the various approximations with the experimental data, once it becomes available, should provide a more sensitive test of the merits of each approximation.

[1]B. L. Moiseiwitsch and S. J. Smith, Rev. Mod. Phys. 40, 238 (1968).
[2]J. F. Williams and B. A. Willis, J. Phys. B 8, 1641 (1975).
[3]W. N. Shelton, E. S. Leherissy, and D. H. Madison, Phys. Rev. A 3, 242 (1971).
[4]W. N. Shelton and J. B. Mix, Phys. Lett. 32A, 285 (1970).
[5]J. N. Gau and J. Macek, Phys. Rev. A 12, 1760 (1975).
[6]M. R. C. McDowell, L. A. Morgan, and V. P. Myerscough, J. Phys. B 8, 1838 (1975).
[7]B. K. Thomas and E. Gerjuoy, J. Math. Phys. 12, 1567 (1971).
[8]L. D. Thomas, G. Csanak, H. S. Taylor, and B. S. Yarlagadda, J. Phys. B 7, 1719 (1974).
[9]S. Geltman and M. B. Hidalgo, J. Phys. B 4, 1299 (1971).
[10]A. E. Kingston, W. C. Fon, and P. G. Burke, J. Phys. B 9, 605 (1976).
[11]P. G. Burke and H. M. Schey, Phys. Rev. 129, 1258 (1962).
[12]M. A. Brandt and D. G. Truhlar, Phys. Rev. A 11, 1340 (1975).
[13]L. S. Rodberg and R. M. Thaler, *Introduction to the Quantum Theory of Scattering* (Academic, New York, 1967), pp. 321–327.
[14]M. L. Goldberger and K. M. Watson, *Collision Theory* (Wiley, New York, 1964), p. 203.
[15]D. H. Madison and W. N. Shelton, Phys. Rev. A 7, 499 (1973).
[16]M. E. Rose, *Elementary Theory of Angular Momentum* (Oxford U. P., London, 1968), p. 192.
[17]Reference 16, Chap. 6, p. 108.
[18]B. V. Noumerov, Monthly Notices Roy. Astron. Soc. 84, 592 (1924).
[19]N. F. Mott and H. S. W. Massey, *The Theory of Atomic Collisions*, 3rd ed. (Clarendon, Oxford, 1965), p. 414.